ACS APPLIED MATERIALS & INTERFACES

Research Article

www.acsami.org

4-(2-Pyridylazo)-resorcinol Functionalized Thermosensitive Ionic Microgels for Optical Detection of Heavy Metal Ions at Nanomolar Level

Xianjing Zhou,[†] Jingjing Nie,[‡] and Binyang Du*[,†]

[†]MOE Key Laboratory of Macromolecular Synthesis and Functionalization, Department of Polymer Science & Engineering, and [‡]Department of Chemistry, Zhejiang University, Hangzhou 310027, China

Supporting Information

ABSTRACT: 4-(2-Pyridylazo)-resorcinol (PAR) functionalized thermosensitive ionic microgels (PAR-MG) were synthesized by a one-pot quaternization method. The PAR-MG microgels were spherical in shape with radius of ca. 166.0 nm and narrow size distribution and exhibited thermo-sensitivity in aqueous solution. The PAR-MG microgels could optically detect trace heavy metal ions, such as Cu^{2+}, Mn^{2+}, Pb^{2+}, Zn^{2+}, and Ni^{2+}, in aqueous solutions with high selectivity and sensitivity. The PAR-MG microgel suspensions exhibited characteristic color with the presence of various trace heavy metal ions, which could be visually distinguished by naked eyes. The limit of colorimetric detection (D_L) was determined to be 38 nM for Cu^{2+} at pH 3, 12 nM for Cu^{2+} at pH 7, and 14, 79, 20, and 21 nM for Mn^{2+}, Pb^{2+}, Zn^{2+}, and Ni^{2+}, respectively, at pH 11, which was lower than (or close to) the United States Environmental Protection Agency standard for the safety limit of these heavy metal ions in drinking water. The mechanism of detection was attributed to the chelation between the nitrogen atoms and *o*-hydroxyl groups of PAR within the microgels and heavy metal ions.

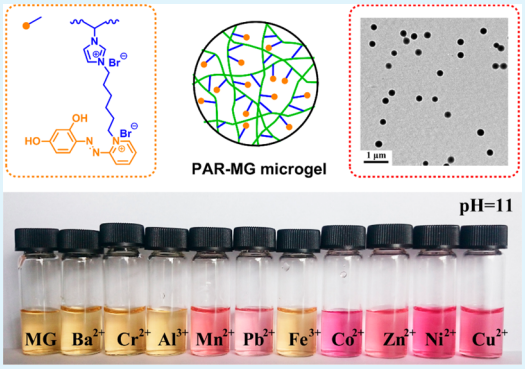

KEYWORDS: *ionic microgels, 4-(2-pyridylazo)-resorcinol, optical detection, heavy metal ion, nanomolar level*

INTRODUCTION

Heavy metal ions are considered as "low density chemical components that are highly toxic".[1] Heavy metal ions are nonbiodegradable and have high solubility in water. The rampant pollution of heavy metal ions in the environment has become a major issue for the countries all over the world due to the fast economic development and human activities, especially for developing countries. Excessive levels of heavy metal ions in aquatic ecosystems and their bioaccumulation over time in organisms can cause great damage to the human health and the environment. It was reported that 19% of groundwater in the United States contains heavy metal ions with concentration above the allowance of the United States Environmental Protection Agency (EPA) human health standard.[2] In China, there were reports about saturnism accidents in local residents due to the pollution of lead ions caused by neighboring storage battery factories. As a result, detection of trace toxic heavy metal ions in water is a target of particular importance for preventing the pollution of heavy metal ions in aquatic ecosystems and protecting human health. It is highly desired and urgent to develop efficient, simple, and inexpensive sensing systems for the detection of trace toxic heavy metal ions in aqueous solutions. Many efforts are devoted to develop new detection strategies like fluorescence,[3−5] colorimetric,[6−9] and quartz crystal microbalance[10] with the use of fluorophors, metal nanoparticles, polymers, and so forth. Among these, colorimetric strategy has attracted considerable attention because it is low cost and suitable for direct real-time and online analysis of heavy metal ions in aqueous solutions.

Microgels are polymeric particles with three-dimensional cross-linked network structures and size ranging from 10 to1000 nm. By properly designing and choosing suitable monomers and comonomers, the resultant microgels could have abilities of responding chemically or physically to the changes in external environment, for example, temperature, pH, ionic strength, solvency, and so forth.[11−17] Because the chemical or physical properties of microgels could be tailored on-demand over a wide range of characteristics, the microgels have wide applications in many technical fields including photochemistry,[18] cosmetics,[19] biomedical applications,[20] catalysts,[21] coating technologies,[22] and sensors.[23] However, the application of microgels in the detection of heavy metal ions in aqueous solution is seldom reported.[24,25] To this end, new functionality is necessarily rendered for the microgels.

In this work, novel functional microgels were designed and synthesized for fast colorimetric detection of various heavy

Received: July 22, 2015
Accepted: September 15, 2015
Published: September 15, 2015

DOI: 10.1021/acsami.5b06653
ACS Appl. Mater. Interfaces 2015, 7, 21966−21974

metal ions, namely, Cu^{2+}, Pb^{2+}, Mn^{2+}, Zn^{2+}, and Ni^{2+}, in aqueous solution at the nanomolar level. Functional thermosensitive ionic microgels were synthesized via a one-pot quaternization reaction during the surfactant free emulsion copolymerization (SFEP) of *N*-isopropylacrylamide (NIPAm) and 1-vinylimidazole (VIM) in the presence of 1,6-dibromohexane and 4-(2-pyridylazo)-resorcinol (PAR), as shown in Scheme 1.[26,27] The hydrophobic indictor, PAR, was

Scheme 1. Synthesis of PAR Functionalized Thermosensitive Ionic Microgels via Quaternization Reaction

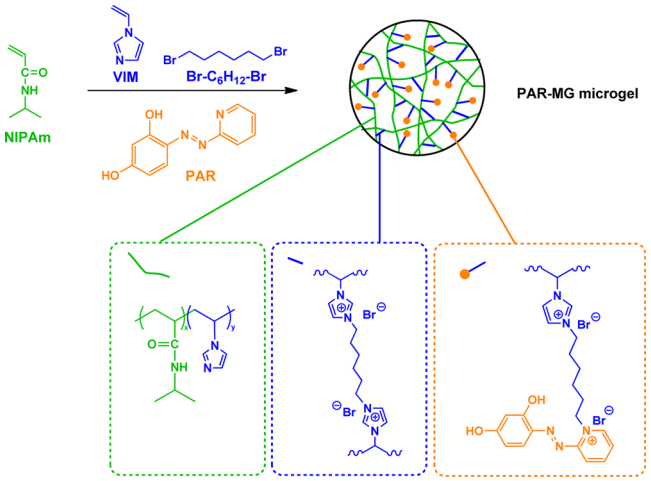

covalently incorporated into the cross-linked network of the microgels via in situ quaternization reaction. PAR is an azo dye widely used as a colorimetric reagent for metal ions because it forms stable chelates with different metal ions.[28] It can also complex with heavy metal ions in polar organic solvent like ethanol.[29−31] By incorporating PAR into the microgel networks, the PAR moieties could then be quickly accessible for the trace heavy metal ions in aqueous solutions because of the colloidal properties and swelling porous structures of the functional microgels, leading to the colorimetric change of the microgel suspensions and the fast detection kinetic and high detection sensitivity. Various trace heavy metal ions in aqueous solutions could be even visually distinguished by naked eyes.

EXPERIMENTAL SECTION

Materials. *N*-Isopropylacrylamide (NIPAm), 1-vinylimidazole (VIM), 2,2′-azobis (2-methylpropionamidine) dihydrochloride (AIBA), 1,6-dibromhexane, 4-(2-pyridylazo)-resorcinol (PAR), *N*,*N*-dimethylformamide (DMF), sodium hydroxide, and hydrogen chloride were used as received without further purification.

Synthesis of PAR Functionalized Thermosensitive Ionic Microgels (PAR-MG). The PAR functionalized thermosensitive ionic microgels (PAR-MG) were prepared via simultaneous quaternized cross-linking reaction during surfactant free emulsion copolymerization (SFEP) of *N*-isopropylacrylamide (NIPAm) as the main monomer and 1-vinylimidazole (VIM) as the comonomer in the presence of 1,6-dibromhexane and 4-(2-pyridylazo)-resorcinol (PAR). Briefly, NIPAm (0.2264 g, 2 mmol) and VIM (27 μL, 0.3 mmol) were added into 45 mL of deionized water at 70 °C under vigorous stirring. Oxygen was eliminated by bubbling nitrogen through the reaction solution for 20 min. Then 5 mL of AIBA aqueous solution (5 mg/mL) was added into the solution to initiate the polymerization. After 10 min, 1 mL of DMF solutions of 1,6-dibromhexane (46 μL, 0.3 mmol) and PAR (64.5 mg, 0. 3 mmol) were dripped slowly into the reaction flask. The reaction was then kept at 70 °C for 6 h. After polymerization, the microgel suspensions were transferred into a dialysis tube with MWCO of 14 000 and dialyzed in DMF for 2 days and in deionized water for 1 week. The DMF was changed every 6 h and deionized water was changed every day.

Normal thermosensitive ionic microgels were also prepared by the same procedure without adding PAR, which were named as N-MG microgels.

Colorimetric Detection of Heavy Metal Ions. Stock salt solutions with concentration of 1 mM were prepared by dissolving the nitric acid salts, that is, Ba^{2+}, Cr^{2+}, Al^{3+}, Mn^{2+}, Pb^{2+}, Fe^{3+}, Co^{2+}, Zn^{2+}, Ni^{2+}, and Cu^{2+} in distilled water. The pH value of the microgel suspensions was adjusted with NaOH or HCl. For colorimetric detection of heavy metal ions, 2 mL suspensions of PAR-MG (C_{MG} = 0.125 mg/mL, C_{PAR} = 0.0046 mg/mL) were filled into a 1 cm quartz cell and given amounts of stock solutions of heavy metal ions were gradually added into the quartz cell by using a micropipet. The total volume of added stock solution of heavy metal ions was less than 20 μL in order to keep the total volume of testing PAR-MG microgel suspensions without obvious change. The color change of PAR-MG microgel suspensions upon adding heavy metal ions was observed qualitatively by naked-eye colorimetric assessment and quantitatively specified by using UV−visible spectrometry.

Characterization. Dynamic light scattering (DLS) of PAR-MG microgels was measured by using a 90 Plus particle size analyzer (Brookhaven Instruments Corp.) at a scattering angle θ of 90° as a function of temperature. The wavelength of laser light λ was 635 nm. The static light scattering (SLS) of PAR-MG microgels was carried out by using a commercial spectrometer ALV-CGS-3 light scattering electronics and multiple tau digital correlater in Changchun Institute

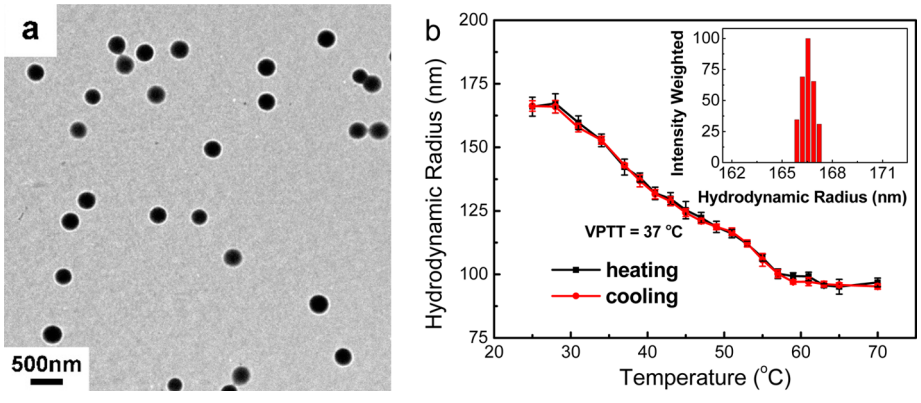

Figure 1. (a) Representative TEM image of PAR-MG microgels and (b) hydrodynamic radius of PAR-MG microgels measured by DLS as a function of measuring temperature. Inset shows the size distribution of PAR-MG microgels at 25 °C.

DOI: 10.1021/acsami.5b06653
ACS Appl. Mater. Interfaces 2015, 7, 21966−21974

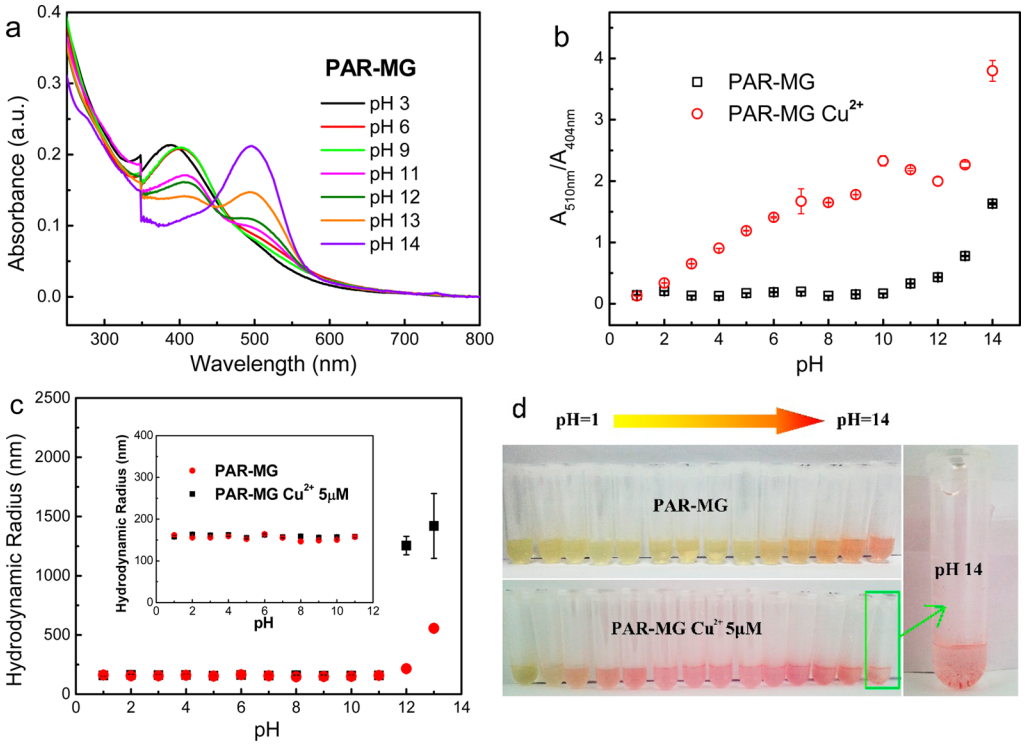

Figure 2. (a) UV−visible absorption spectra of PAR-MG microgels with concentration of 0.05 mg/mL at various pH values. (b) A_{510nm}/A_{404nm} ratio as a function of pH for PAR-MG microgel suspensions without or with the presence of 5 μM Cu^{2+}. (c) Hydrodynamic radii of PAR-MG microgels as a function of pH without or with the presence of 5 μM Cu^{2+}. (d) Photographs of PAR-MG microgels without or with 5 μM Cu^{2+} at different pH values.

of Applied Chemistry, Chinese Academy of Sciences. The SLS measurements were performed at 25 °C, and the sample solutions were equilibrated for 15 min. The range of scattering angle θ used for SLS was from 35° to 135° with a step of 5°. The wavelength of laser light λ was 632.8 nm. Transmission electron microscopy (TEM) measurements were carried out with a HT-7700 electron microscope operated at an acceleration voltage of 100 kV. The TEM samples were prepared by dip-coating with Formvar-coated copper grids into the microgel suspensions. The grids were allowed to dry in air at room temperature before observation. UV−visible spectra were recorded on a Cary 300 instrument (Varian Australia Pty Ltd.). The pH values of sample solutions were measured with a pH meter (FE20, METTLER TOLEDO).

RESULTS AND DISCUSSION

Synthesis of PAR Functionalized Thermosensitive Ionic Microgels. As shown in Scheme 1, 4-(2-pyridylazo)-resorcinol (PAR) functionalized thermosensitive ionic microgels named as PAR-MG microgels were successfully obtained via the simultaneous quaternized cross-linking reaction during the surfactant free emulsion copolymerization (SFEP) of *N*-isopropylacrylamide (NIPAm) as the main monomer, 1-vinylimidazole (VIM) as the comonomer, and 1,6-dibromohexane as the cross-linker with the presence of PAR. PAR with tertiary amine group was successfully incorporated into the cross-linking network of obtained microgels via quaternization reaction. One 1,6-dibromohexane molecule could quaternize two VIM molecules, leading to the formation of cross-linking network. On the other hand, 1,6-dibromohexane molecule could quaternize with one VIM molecule and one PAR molecule, leading to the incorporation of PAR within the resultant microgels. Figure 1a shows the representative TEM image of obtained PAR-MG microgels, which were spherical in shape with a narrow size distribution. The average radius was about 142 ± 12 nm as calculated from the TEM image. The PAR-MG microgels exhibited thermosensitive character because of the use of NIPAm, as shown in Figure 1b. The hydrodynamic radius of PAR-MG microgels decreased with increasing the solution temperature. With raising the solution temperature, the poly(*N*-isopropylacrylamide) (PNIPAm) segments became hydrophobic and insoluble in aqueous solution, leading to the shrinking and collapse of microgels at high temperature. The PAR-MG microgels displayed a very broad transition temperature range from 28 to 55 °C, which was quite different from that of PNIPAm microgels. The volume phase transition temperature (VPTT) of PAR-MG microgels could be determined from plots of the first-order derivative of the hydrodynamic radius versus temperature, because the largest change in R_h occurred when the transition was at a maximum.[32] The VPTT of PAR-MG microgels was ca. 37 °C, which was higher than that of ∼32 °C for linear PNIPAm in aqueous solution.[33] The copolymerization with hydrophilic comonomer VIM and the charged quaternary ammonium salts shifted the VPTT of PAR-MG microgels to higher temperature. The broad transition temperature range can be related to heterogeneous distribution of the hydrophobic PAR segments and hydrophilic polymer segments as well as charged quaternary VIM. The thermosensitive behavior of PAR-MG microgels was reversible. The inset of Figure 1b shows the size distribution of PAR-MG microgels at 25 °C as measured by DLS, which further confirmed that the obtained PAR-MG microgels were with narrow size distribution. The hydrodynamic radius R_h of PAR-MG microgels measured by DLS at 25 °C was 166 ± 4 nm, which was slightly larger than the average radius calculated from TEM images (i.e., 142 ± 12 nm). It was reasonable because

DOI: 10.1021/acsami.5b06653
ACS Appl. Mater. Interfaces 2015, 7, 21966−21974

hydrodynamic radius R_h represented the sizes of fully swollen microgels while TEM results reflected the sizes of adsorbed microgels drying by solvent evaporation. It was also understandable that the TEM size of adsorbed microgels would be larger than the hydrodynamic radius of microgels at higher temperature, which were completed collapsed. However, for the adsorbed microgels on copper grids, they were partially collapsed after drying.

The radius of gyration $\langle R_g \rangle$ of the PAR-MG microgels was also measured by SLS at 25 °C. The $\langle R_g \rangle$, $\langle R_h \rangle$, and corresponding ratio of $\langle R_g \rangle / \langle R_h \rangle$ for the PAR-MG microgels at 25 °C were 126.3 nm, 166.0 nm, and 0.761, respectively. The value of $\langle R_g \rangle / \langle R_h \rangle$ could reflect the cross-linking density distribution of the microgels.[34,35] For uniform hard spheres, $\langle R_g \rangle / \langle R_h \rangle$ is 0.778. For thermosensitive PNIPAm microgels with inhomogeneous cross-linking network structures, $\langle R_g \rangle / \langle R_h \rangle$ usually had the value of 0.55−0.96.[35−38] The $\langle R_g \rangle / \langle R_h \rangle$ value of 0.761 for the PAR-MG microgels was close to that of uniform hard spheres, indicating that the cross-linking network structure of PAR-MG microgels was homogeneous.

The PAR-MG microgel suspensions exhibited characteristic adsorption peak at 404 nm by UV−visible spectroscopy (Figure S1a), indicating the successful incorporation of PAR moieties. The PAR contents of PAR-MG microgels were determined to be ca. 3.7 wt % based on the intensity of adsorption peak at 404 nm by referring to the standard curve of PAR in DMF (Figure S1b). Note that the reference was the N-MG microgels with the same concentration, which showed not any adsorption peak.

Colorimetric Detection of Heavy Metal Ions. We first explored the effect of pH on the change of color and hydrodynamic radius of PAR-MG microgels without and with the presence of Cu^{2+}. Note that the concentration of PAR-MG microgels was 0.05 mg/mL. With increasing pH from 1 to 14 for PAR-MG microgel suspensions, the absorption peak at 389 nm slightly shifted to 404 nm at pH 6, the absorption peak at 404 nm gradually weakened and eventually disappeared at pH 14, and a new absorption peak at 510 nm started to clearly appear for pH above 11, as shown in Figure 2a. Figure 2b shows the intensity ratio of A_{510nm}/A_{404nm} for the adsorption peaks at 510 and 404 nm at various pH values. Strong increase of A_{510nm}/A_{404nm} was observed for pH above 11. Below pH 11, the value of A_{510nm}/A_{404nm} was almost unchanged. The evolution of UV adsorption peak at different pH value is reasonable because PAR is a dibasic acid.[39] With increasing the pH value of aqueous solution, the *p*-hydroxyl group [pK_{OH} (*p*) = 5.6] is first deprotonated and the *o*-hydroxyl group [pK_{OH} (*o*) = 11.9] is second deprotonated in basic medium because the *o*-hydroxyl proton is hydrogen bonded to the azo group,[40] as shown in Figure S2. Therefore, with increasing the pH value to 6, the *p*-hydroxyl group is ionized to be oxygen ion, leading to the increase of electron density of conjugated system and slight bathochromic shift. When the pH value is increased above 11, the *o*-hydroxyl group is deprotonated with the rupture of hydrogen bond, leading to a stronger delocalization of electrons in the conjugated system of PAR and a bathochromic shift.[41,42] Figure 2c shows that the hydrodynamic radii of PAR-MG microgels were unchanged for pH from 1 to 11 as measured by DLS. The color of PAR-MG microgel suspensions changed from yellow to orange with pH above 11, as shown in Figure 2d. Interestingly, the value of A_{510nm}/A_{404nm} increased almost linearly with increasing pH value from 1 to 11 with the presence of 5 μM Cu^{2+} (Figure 2b). The original UV−visible spectra of PAR-MG microgel suspensions with the presence of 5 μM Cu^{2+} at various pH values were shown in Figure S3. With 5 μM Cu^{2+}, the color of PAR-MG microgel suspensions changed from yellow to pink for pH > 2 (Figure 2d). As reported in the literature, PAR chelated with metals through the pyridine nitrogen atom, the azo nitrogen farthest from the heterocyclic ring, and the *o*-hydroxyl group to form two stable 5-membered chelate ring.[28] For our system, the pyridine nitrogen atom of PAR had been quaternized so that only the azo nitrogen and the *o*-hydroxyl group of PAR could chelate metal ions. The formation of complexes would enhance the rigidity of PAR, which resulted in the more stable planar structure and stronger conjugation. That is why the absorption peak showed bathochromic shift and the color changed from yellow to pink. However, the hydrodynamic radii of PAR-MG microgels with Cu^{2+} did not change until the pH value was 12 (Figure 2c). When the pH reached 14, the PAR-MG microgels precipitated with the presence of 5 μM Cu^{2+} (Figure 2d). These results show that the colorimetric behavior and particle size of PAR-MG microgels were unaffected in a wide range of pH from 1 to 10. However, the complexation between heavy metal ionic and PAR-MG microgels occurred in a wide range of pH from 1 to 14. Therefore, the pH 3, 7, and 11 were chosen for further detail investigation of detecting trace heavy metal ions with PAR-MG microgels.

We also studied the effect of concentration of PAR-MG microgels on the change of A_{510nm}/A_{404nm} ratio with the presence of Cu^{2+} at pH 7. We chose five different concentrations, that is, 0.05, 0.0625, 0.075, 0.1, and 0.125 mg/mL, respectively. Figure 3 shows the A_{510nm}/A_{404nm} ratio as a function of $[Cu^{2+}]/[PAR]$ for PAR-MG microgel suspensions with different concentrations. Note that $[Cu^{2+}]/[PAR]$ represented the ratio of molar concentration for Cu^{2+} to PAR in the PAR-MG microgel suspensions. The intensity ratio of A_{510nm}/A_{404nm} first increased with increasing the concentration of Cu^{2+} and reached a plateau value when the value of $[Cu^{2+}]/[PAR]$ reached ca. 0.75 for all concentrations of PAR-MG microgels. The nonlinear nature of the A_{510nm}/A_{404nm} curve at higher concentrations is due to the saturation effects.[43] Thus, within a certain range, the concentration of PAR-MG microgels did not affect the complexation behavior between PAR and Cu^{2+}. For our system, on one hand, the pyridine nitrogen atom of PAR had been quaternized so that only the azo nitrogen and the *o*-hydroxyl group of PAR could chelate Cu^{2+}; on the other hand, amide group of NIPAm could also participate in the formation

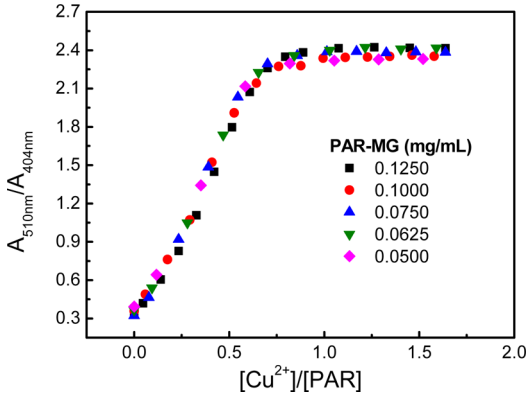

Figure 3. A_{510nm}/A_{404nm} ratio as a function of $[Cu^{2+}]/[PAR]$ for PAR-MG microgel suspensions with different concentrations at pH 7.

DOI: 10.1021/acsami.5b06653
ACS Appl. Mater. Interfaces 2015, 7, 21966−21974

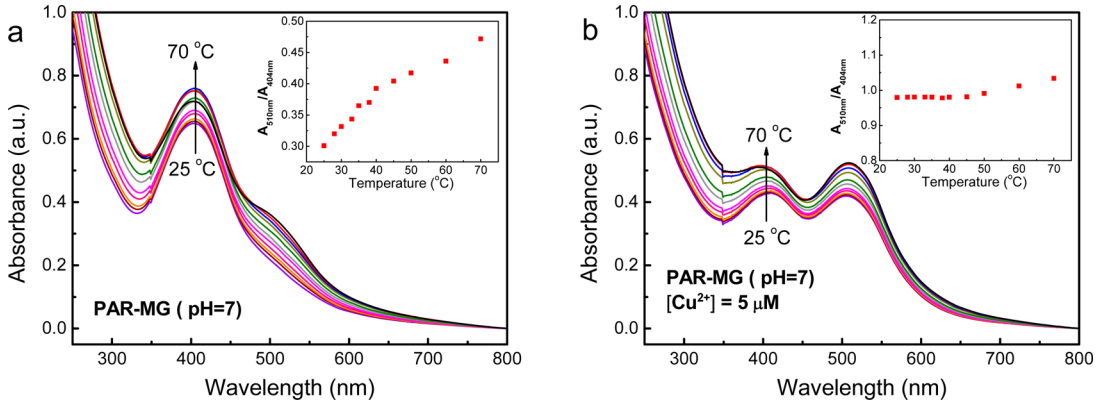

Figure 4. UV−visible spectra of PAR-MG microgels at various temperatures and pH 7 without (a) or with (b) the presence of 5 μM Cu^{2+}. Insets show the corresponding A_{510nm}/A_{404nm} ratio as a function of measuring temperature. The concentration of PAR-MG microgels was 0.05 mg/mL.

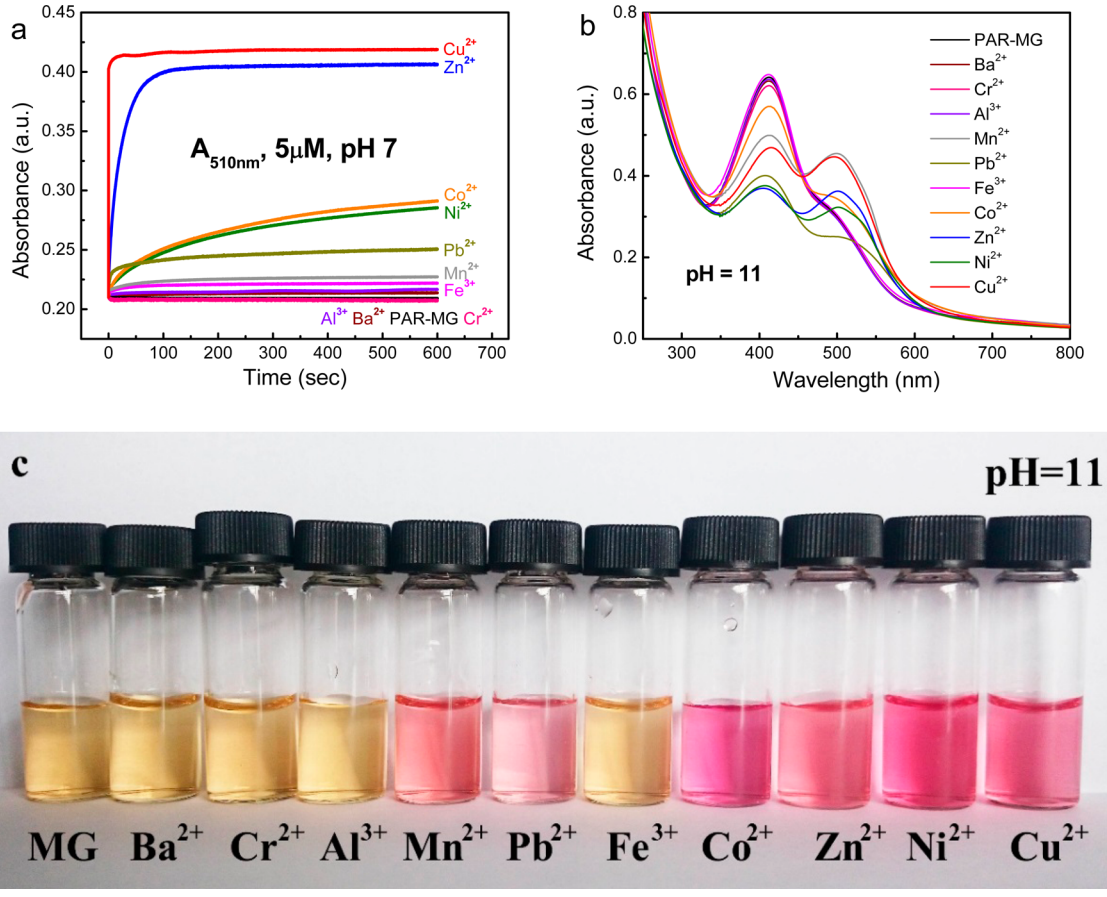

Figure 5. (a) Intensity evolution of UV absorption peak at 510 nm for PAR-MG microgel suspensions at pH 7 with the presence of various heavy metal ions (5 μM) as a function of time. (b) UV−vis adsorption spectra of PAR-MG microgel suspensions with the presence of different heavy metal ions (5 μM) at pH 11. (c) Digital photograph of PAR-MG microgel suspensions with the presence of 5 μM various heavy metal ions at pH 11. The concentration of PAR-MG microgels was 0.125 mg/mL.

of complex with Cu^{2+}. Moreover, the steric effects and immobilizing of PAR within the cross-linked networks of microgels might also result in the complexation of more than one PAR with Cu^{2+}. Figure S4 shows the possible complex structures of PAR with Cu^{2+}. One Cu^{2+} could complex with one, two, or three PAR structures, leading to the value of $[Cu^{2+}]/[PAR]$ to be 1, 0.5, and 0.33, respectively. As resulted in Figure 3a, the intensity ratio of A_{510nm}/A_{404nm} became saturated when the value of $[Cu^{2+}]/[PAR]$ reached ca. 0.75, so one Cu^{2+} could be more likely to complex with one or two PAR structures in our system.

As mentioned above, the PAR-MG microgels exhibited thermosensitive property. We further investigated the effects of temperature on their detection of heavy metal ions. Figure 4 shows the UV−visible spectra of PAR-MG microgels at various temperatures without or with the presence of 5 μM Cu^{2+}. It can be seen that the A_{510nm}/A_{404nm} ratio of PAR-MG microgels without Cu^{2+} increased with increasing the measuring temperature (Figure 4a). With increasing temperature, the hydrogen

DOI: 10.1021/acsami.5b06653
ACS Appl. Mater. Interfaces 2015, 7, 21966−21974

bonds between *o*-hydroxyl proton and azo group in PAR structure will be broken, leading to the increase of electron density of conjugated system and bathochromic shift. Furthermore, the increase of absolute adsorption intensity was also partially attributed to the shrink of PAR-MG microgels at higher temperature, which led to the decrease of transmission of light. However, for PAR-MG microgels with the presence of Cu^{2+}, the temperature did not affect the colorimetric behavior when the measuring temperatures were in the range of 25−50 °C except for the increase of absolute intensity. The A_{510nm}/A_{404nm} ratio was kept unchanged in the temperature range of 25−50 °C. With further increasing the temperature up to 70 °C, the A_{510nm}/A_{404nm} ratio increased slightly. Because the PAR-MG microgels collapsed at high temperature above its VPTT (37 °C) in aqueous solution, it would be better to apply such microgels at temperature lower than its VPTT for the detection of heavy metal ions in aqueous solution.

To determine the detection kinetics, the UV−vis spectra of PAR-MG microgel suspensions at pH 7 with the presence of various heavy metal ions, that is, Ba^{2+}, Cr^{2+}, Al^{3+}, Mn^{2+}, Pb^{2+}, Fe^{3+}, Co^{2+}, Zn^{2+}, Ni^{2+}, and Cu^{2+}, were recorded for different time periods. Note that the concentration of heavy metal ions was 5 μM and the concentration of PAR-MG microgels was 0.125 mg/mL. The addition of 5 μM heavy metal ions led to the increase of absorption intensity at 510 nm, which reached maximum within 600 s, as shown in Figure 5a. The detection kinetics of PAR-MG microgels in response to heavy metal ions Mn^{2+}, Pb^{2+}, Zn^{2+}, Ni^{2+}, and Cu^{2+} at pH 3 and pH 11 were also investigated and are shown in Figure S5. The results of Figures 5a and S5 indicate that PAR-MG microgels could completely complex with the heavy metal ions within 600 s, which was then chosen as the responding time for the detection of heavy metal ions. After complexing with heavy metal ions, the hydrodynamic radii of PAR-MG microgels did not change much, as shown in Figure S6. However, the UV−vis adsorption spectra of PAR-MG microgel suspensions with the presence of different heavy metal ions were different and dependent on the pH values, as shown in Figures 5b and S7. As a result, the PAR-MG microgel suspensions exhibited different colors for different heavy metal ions at pH 3, 7, and 11. The heavy metal ions with unoccupied orbitals could coordinate with azo nitrogen and *o*-hydroxyl group of PAR. There are some types of electronic transitions commonly observed in coordination compounds, that is, metal-centered (MC), ligand-centered (LC), ligand-to-metal chargetransfer (LMCT), and metal-to-ligand charge-transfer (MLCT) transitions.[44,45] Different metal ions have different valence electron structures, ionic radii, or unoccupied orbitals, which could cause different ligand field transition or charge transfer. These might be the reasons why the absorption peak positions of PAR-MG complexed with different metals are slightly different. In addition, at different pH values, hydrogen ions or hydroxide ions in the solutions would have competition or promotion for complexing of metals and ligands. It is a complicated dynamic equilibrium process so that the PAR-MG microgel suspensions exhibited different colors with the presence of different heavy metal ions at different pH. Simulation and theoretical considerations like quantum chemical calculation are needed for quantitative understanding the complex mechanism between PAR and the metal ions as well as their pH and ion dependence. Figure 5c shows the representative digital photographs of PAR-MG microgel suspensions at pH 11 with the presence of different heavy metal ions with concentration of 5 μM. Clearly, one can visually distinguish the type of heavy metal ions from the color of PAR-MG microgel suspensions by naked eyes. The digital photographs of PAR-MG microgel suspensions at pH 3 and pH 7 after adding 5 μM corresponding heavy metal ions are shown in Figure S7c and d. The responses of PAR-MG microgels to common ions (i.e., K^+, Na^+, Ca^{2+}, and Mg^{2+}) were also investigated, as shown in Figure S7b. The UV−vis adsorption spectra did not change after adding K^+, Na^+, Ca^{2+}, or Mg^{2+}, which were consistent with literature report.[42]

The selectivity of the PAR-MG microgels toward various heavy metal ions was investigated. Although the UV−vis adsorption spectra of PAR-MG microgel suspensions with the presence of different heavy metal ions were different and dependent on the pH values, the intensity ratio of A_{510nm}/A_{404nm} was again taken for comparison. Figure 6 shows the

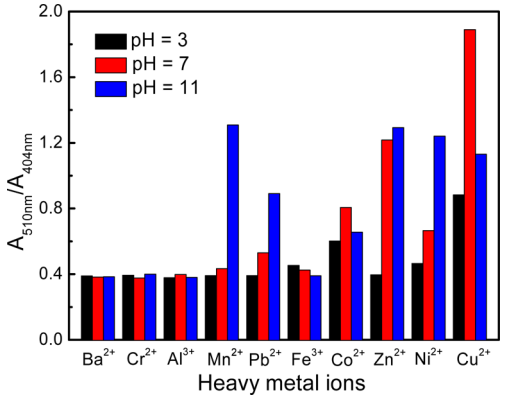

Figure 6. Intensity ratios of A_{510nm}/A_{404nm} for PAR-MG microgel suspensions at different pH values after adding various heavy metal ions, that is, Ba^{2+}, Cr^{2+}, Al^{3+}, Mn^{2+}, Pb^{2+}, Fe^{3+}, Co^{2+}, Zn^{2+}, Ni^{2+}, and Cu^{2+}, with concentration of 9 μM. Note that the concentration of PAR-MG microgels was 0.125 mg/mL.

A_{510nm}/A_{404nm} value for PAR-MG microgel suspensions after adding various heavy metal ions, that is, Ba^{2+}, Cr^{2+}, Al^{3+}, Mn^{2+}, Pb^{2+}, Fe^{3+}, Co^{2+}, Zn^{2+}, Ni^{2+}, and Cu^{2+}, with concentration of 9 μM at pH 3, 7, and 11. Note that the concentration of PAR-MG microgels was 0.125 mg/mL. It can be seen that for, Ba^{2+}, Cr^{2+}, and Al^{3+}, A_{510nm}/A_{404nm} value was the same as that of pure PAR-MG microgel suspensions regardless of pH value. In other words, the PAR-MG microgels did not respond to Ba^{2+}, Cr^{2+}, and Al^{3+}. Furthermore, the A_{510nm}/A_{404nm} values for other heavy metal ions were dependent on the pH value of PAR-MG microgel suspensions. Clearly, PAR-MG microgels could responsd to Mn^{2+}, Pb^{2+}, and Ni^{2+} only at pH 11. Zn^{2+} could complex with PAR-MG microgels at pH 7 and 11. For Cu^{2+} and Co^{2+}, they could complex with PAR-MG microgels at pH 3, 7, and 11.

The above results indicated that the PAR-MG microgels exhibited excellent selectivity toward Cu^{2+} over other competitive metal ions at pH 3. Figure 7a shows the A_{510nm}/A_{404nm} ratios of PAR-MG microgels at pH 3 after each addition step of various metal ions. Note that the concentration of each metal ion was 5 μM. The adding sequence of metal ions was Ba^{2+}, Cr^{2+}, Al^{3+}, Mn^{2+}, Pb^{2+}, Fe^{3+}, Co^{2+}, Zn^{2+}, Ni^{2+}, K^+, Na^+, Ca^{2+}, Mg^{2+}, and Cu^{2+}. The copresence of other metal ions did not affect the selectively and sensitivity of PAR-MG microgels toward Cu^{2+}. The previous addition of other metal ions only led to slight bathochromic shift of the adsorption peak of PAR-

DOI: 10.1021/acsami.5b06653
ACS Appl. Mater. Interfaces 2015, 7, 21966−21974

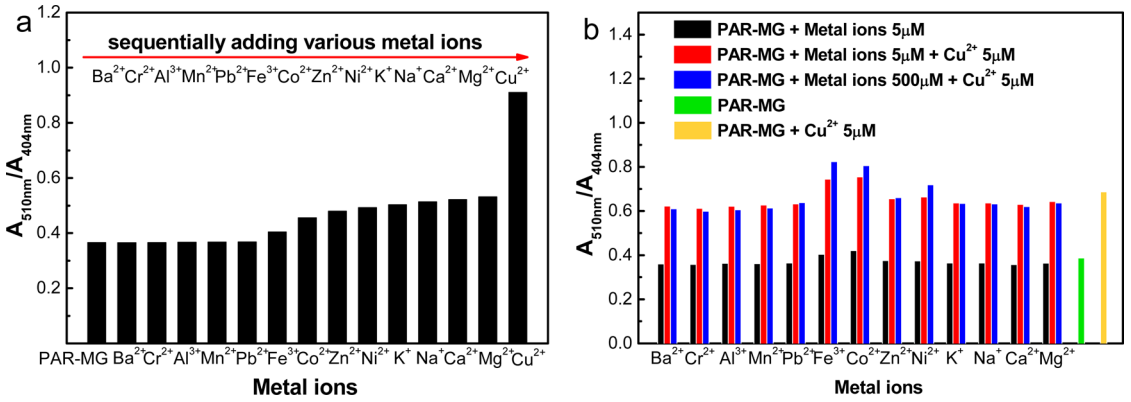

Figure 7. (a) A_{510nm}/A_{404nm} ratios of PAR-MG microgels at pH 3 after sequential addition of various metal ions. The addition sequence of metal ions was Ba^{2+}, Cr^{2+}, Al^{3+}, Mn^{2+}, Pb^{2+}, Fe^{3+}, Co^{2+}, Zn^{2+}, Ni^{2+}, K^{+}, Na^{+}, Ca^{2+}, Mg^{2+}, and Cu^{2+}. The concentrations of PAR-MG microgels and each metal ion were 0.125 mg/mL and 5 μM, respectively. (b) Interference studies of different metal ions on detection ability of PAR-MG microgels for Cu^{2+} at pH 3. The concentration of Cu^{2+} was 5 μM.

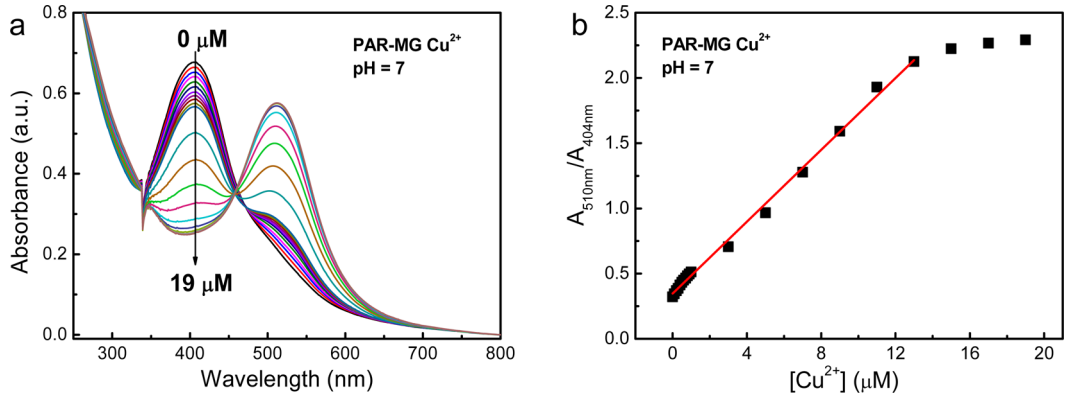

Figure 8. (a) UV−vis adsorption spectra of PAR-MG microgel suspensions at pH 7 by sequenced addition of Cu^{2+}. (b) Intensity ratio of A_{510nm}/A_{404nm} of PAR-MG microgel suspensions at pH 7 as a function of Cu^{2+} concentrations. The concentration of PAR-MG microgels was 0.125 mg/mL.

MG microgels after adding Fe^{3+} and Co^{2+}. The final addition of Cu^{2+} led to the significant increasing of A_{510nm}/A_{404nm} ratio. Interference studies of different metal ions on detection ability of PAR-MG microgels for Cu^{2+} at pH 3 were also studied. Figure 7b shows the changes of A_{510nm}/A_{404nm} ratios of PAR-MG microgels at pH 3 containing 5 μM Cu^{2+} in the presence of various interfering ions with concentrations of 5 μM and 500 μM, respectively. It can be seen from Figure 7b that only Fe^{3+} and Co^{2+} caused some interference at 5 μM. However, at higher concentration of 500 μM, not only Fe^{3+} and Co^{2+} but also Ni^{2+} exhibited some interference.

Basing on the results of Figures 5−7, the responses of PAR-MG microgels to Cu^{2+} at pH 3 and 7, and Mn^{2+}, Pb^{2+}, Zn^{2+}, and Ni^{2+} at pH 11 were further investigated to determine the detection sensitivity of PAR-MG microgels for these heavy metal ions. Figure 8a shows the evolution of UV−vis adsorption spectra of PAR-MG microgel suspensions at pH 7 by sequenced addition of Cu^{2+}. The intensity ratio of A_{510nm}/A_{404nm} first increased linearly with increasing the concentration of Cu^{2+} and reached a plateau value for $[Cu^{2+}]$ larger than 15 μM (Figure 8b). A linear relationship was found to be $Y = 0.138[Cu^{2+}] + 0.347$ for $[Cu^{2+}]$ in the range of 0−13 μM with R^2 value of 0.997. In other words, trace Cu^{2+} in aqueous solutions with concentrations of 0−13 μM could be accurately detected by PAR-MG microgels with the association constant of 0.138 μM^{-1}. Note that if the heavy metal ions had higher concentration above a certain micromolar, the PAR-MG microgels were not able to monitor such high concentration of metal ions. The limits of detection (D_L) for PAR-MG microgels in the detection of heavy metal ions, Cu^{2+} could be calculated from the data in the linear range (Figure 8b), according to the 3α IUPAC criteria:[5,46]

$$D_L = \frac{kS_b}{m} \quad (1)$$

where k is a factor with the value of 3, S_b is the standard deviation of the blank, and m is the slope of the calibration graph in the linear range. The S_b was 0.084% from five successive blank measurements. D_L was then calculated to be 12 nM for Cu^{2+} at pH 7, which was nearly 2000 times lower than the maximum level of Cu^{2+} (i.e., ∼ 20 μM) in drinking water permitted by the United States. EPA.[47] Similar phenomena were observed for detecting Cu^{2+} at pH 3 and Mn^{2+}, Pb^{2+}, Zn^{2+}, and Ni^{2+} at pH 11, as shown in Figures S8−S12. The values of D_L for PAR-MG microgels in the detection of heavy metal ions, Cu^{2+} at pH 3 and Mn^{2+}, Zn^{2+}, and Ni^{2+} at pH 11, were determined to be 38, 14, 20, and 21 nM, respectively, which were lower than the United States EPA standard for the safety limit of Cu^{2+}, Mn^{2+}, Zn^{2+}, and Ni^{2+} in drinking water. For Pb^{2+} at pH 11, D_L was 79 nM, which was close to the United States EPA standard for the safety limit of Pb^{2+} in drinking water. Note that the EPA standard set the maximum level of Mn^{2+}, Pb^{2+}, Zn^{2+}, and Ni^{2+} in drinking water

DOI: 10.1021/acsami.5b06653
ACS Appl. Mater. Interfaces 2015, 7, 21966−21974

to about 909 nM (i.e.50 μg/L), 72 nM (i.e., 15 μg/L), 76 μM (5 mg/L), and 680 nM (40 μg/L), respectively.[47,48]

CONCLUSIONS

4-(2-Pyridylazo)-resorcinol (PAR) functional microgels were designed and successfully synthesized by a one-pot quaternization reaction for fast colorimetric detection of various heavy metal ions in aqueous solution at nanomolar level. The PAR-MG microgels were spherical in shape with narrow size distribution. The microgels could optically detect trace heavy metal ions in aqueous solutions, and especially exhibit high sensitivity and excellent selectivity toward Cu^{2+} over other metal ions under strongly acidic conditions (pH 3). The limit of colorimetric detection was determined to be 38 nM for Cu^{2+} at pH 3, 12 nM for Cu^{2+} at pH 7, and 14, 79, 20, and 21 nM for Mn^{2+}, Pb^{2+}, Zn^{2+}, and Ni^{2+}, respectively, at pH 11. The PAR-MG microgels also exhibited characteristic color with the presence of various trace heavy metal ions, which could be visually distinguished by naked eyes.

ASSOCIATED CONTENT

Supporting Information

The Supporting Information is available free of charge on the ACS Publications website at DOI: 10.1021/acsami.5b06653.

Additional UV−visible absorption spectrum, DLS data, and photographs of PAR-MG microgel suspensions with the presence of various heavy metal ions at various pH values (PDF)

AUTHOR INFORMATION

Corresponding Author

*E-mail: duby@zju.edu.cn.

Notes

The authors declare no competing financial interest.

ACKNOWLEDGMENTS

The authors thank the National Natural Science Foundation of China (Nos. 21274129 and 21322406), the Fundamental Research Funds for the Central Universities (2014XZZX003-21), the third level of 2013 Zhejiang Province 151 Talent Project, and Open Research Fund of State Key Laboratory of Polymer Physics and Chemistry, Changchun Institute of Applied Chemistry, Chinese Academy of Sciences for financial support.

REFERENCES

(1) Tekaya, N.; Saiapina, O.; Ben Ouada, H.; Lagarde, F.; Ben Ouada, H.; Jaffrezic-Renault, N. Ultra-Sensitive Conductometric Detection of Heavy Metals Based on Inhibition of Alkaline Phosphatase Activity from Arthrospira Platensis. *Bioelectrochemistry* **2013**, *90*, 24−29.

(2) Joseph D, A.; Jo Ann M, G.; Lori E, A. *Trace Elements and Radon in Groundwater Across the United States, 1992−2003*; U.S. Geological Survey, Reston, VA, 2011.

(3) Yin, M.; Li, Z.; Liu, Z.; Yang, X.; Ren, J. Magnetic Self-Assembled Zeolite Clusters for Sensitive Detection and Rapid Removal of Mercury(II). *ACS Appl. Mater. Interfaces* **2012**, *4*, 431−437.

(4) Yuen, L. H.; Franzini, R. M.; Tan, S. S.; Kool, E. T. Large-Scale Detection of Metals with a Small Set of Fluorescent DNA-Like Chemosensors. *J. Am. Chem. Soc.* **2014**, *136*, 14576−14582.

(5) Zhang, K.; Guo, J.; Nie, J.; Du, B.; Xu, D. Ultrasensitive and Selective Detection of Cu^{2+} in Aqueous Solution with Fluorescence Enhanced CdSe Quantum Dots. *Sens. Actuators, B* **2014**, *190*, 279−287.

(6) Huang, C. C.; Chang, H. T. Parameters for Selective Colorimetric Sensing of Mercury(II) in Aqueous Solutions Using Mercaptopropionic Acid-Modified Gold Nanoparticles. *Chem. Commun.* **2007**, *12*, 1215−1217.

(7) Zhang, M.; Liu, Y. Q.; Ye, B. C. Colorimetric Assay for Parallel Detection of Cd^{2+}, Ni^{2+} and Co^{2+} using Peptide-Modified Gold Nanoparticles. *Analyst* **2012**, *137*, 601−607.

(8) Dwivedi, C.; Chaudhary, A.; Gupta, A.; Nandi, C. K. Direct Visualization of Lead Corona and Its Nanomolar Colorimetric Detection Using Anisotropic Gold Nanoparticles. *ACS Appl. Mater. Interfaces* **2015**, *7*, 5039−5044.

(9) Gogoi, N.; Barooah, M.; Majumdar, G.; Chowdhury, D. Carbon Dots Rooted Agarose Hydrogel Hybrid Platform for Optical Detection and Separation of Heavy Metal Ions. *ACS Appl. Mater. Interfaces* **2015**, *7*, 3058−3067.

(10) Cao, Z.; Guo, J.; Fan, X.; Xu, J.; Fan, Z.; Du, B. Detection of Heavy Metal Ions in Aqueous Solution by P(MBTVBC-co-VIM)-Coated QCM Sensor. *Sens. Actuators, B* **2011**, *157*, 34−41.

(11) Seiffert, S. Microgel Capsules Tailored by Droplet-Based Microfluidics. *ChemPhysChem* **2013**, *14*, 295−304.

(12) Bonham, J. A.; Faers, M. A.; van Duijneveldt, J. S. Non-Aqueous Microgel Particles: Synthesis, Properties and Applications. *Soft Matter* **2014**, *10*, 9384−9398.

(13) Liu, H.; Wei, Z.; Hu, M.; Deng, Y.; Tong, Z.; Wang, C. Fabrication of Degradable Polymer Microspheres via pH-Responsive Chitosan-Based Pickering Emulsion Photopolymerization. *RSC Adv.* **2014**, *4*, 29344−29351.

(14) Sigolaeva, L. V.; Gladyr, S. Y.; Gelissen, A. P. H.; Mergel, O.; Pergushov, D. V.; Kurochkin, I. N.; Plamper, F. A.; Richtering, W. Dual-Stimuli-Sensitive Microgels as a Tool for Stimulated Spongelike Adsorption of Biomaterials for Biosensor Applications. *Biomacromolecules* **2014**, *15*, 3735−3745.

(15) Yang, Q.; Wang, K.; Nie, J.; Du, B.; Tang, G. Poly(N-vinylpyrrolidinone) Microgels: Preparation, Biocompatibility, and Potential Application as Drug Carriers. *Biomacromolecules* **2014**, *15*, 2285−2293.

(16) Wang, W.; Milani, A. H.; Carney, L.; Yan, J.; Cui, Z.; Thaiboonrod, S.; Saunders, B. R. Doubly Crosslinked Microgel-Colloidosomes: a Versatile Method for pH-Responsive Capsule Assembly Using Microgels as Macro-Crosslinkers. *Chem. Commun.* **2015**, *51*, 3854−3857.

(17) Kuckling, D.; Vo, C. D.; Wohlrab, S. E. Preparation of Nanogels with Temperature-Responsive Core and pH-Responsive Arms by Photo-Cross-Linking. *Langmuir* **2002**, *18*, 4263−4269.

(18) Sasa, N.; Yamaoka, T. Surface Activated Photopolymer Microgels. *Adv. Mater.* **1994**, *6*, 417−421.

(19) Gichinga, M. G.; Striegler, S.; Dunaway, N. A.; Barnett, J. D. Miniemulsion Polymers as Solid Support for Transition Metal Catalysts. *Polymer* **2010**, *51*, 606−615.

(20) Supasuteekul, C.; Milani, A. H.; Saunders, J. M.; Lally, S.; Freemont, T.; Saunders, B. R. A Study of Hydrogel Composites Containing pH-Responsive Doubly Crosslinked Microgels. *Soft Matter* **2012**, *8*, 7234−7242.

(21) Mei, Y.; Lu, Y.; Polzer, F.; Ballauff, M.; Drechsler, M. Catalytic Activity of Palladium Nanoparticles Encapsulated in Spherical Polyelectrolyte Brushes and Core-Shell Microgels. *Chem. Mater.* **2007**, *19*, 1062−1069.

(22) Butun, V.; Atay, A.; Tuncer, C.; Bas, Y. Novel Multiresponsive Microgels: Synthesis and Characterization Studies. *Langmuir* **2011**, *27*, 12657−12665.

(23) Scheffold, F.; Diaz-Leyva, P.; Reufer, M.; Ben Braham, N.; Lynch, I.; Harden, J. L. Brushlike Interactions Between Thermoresponsive Microgel Particles. *Phys. Rev. Lett.* **2010**, *104*, 128304.

(24) Yin, J.; Guan, X.; Wang, D.; Liu, S. Metal-Chelating and Dansyl-Labeled Poly(N-isopropylacrylamide) Microgels as Fluorescent Cu^{2+} Sensors with Thermo-Enhanced Detection Sensitivity. *Langmuir* **2009**, *25*, 11367−11374.

(25) Helwa, Y.; Dave, N.; Froidevaux, R.; Samadi, A.; Liu, J. Aptamer-Functionalized Hydrogel Microparticles for Fast Visual Detection of

DOI: 10.1021/acsami.5b06653
ACS Appl. Mater. Interfaces 2015, 7, 21966−21974

Mercury(II) and Adenosine. *ACS Appl. Mater. Interfaces* **2012**, *4*, 2228−2233.
(26) Zhou, X.; Zhou, Y.; Nie, J.; Ji, Z.; Xu, J.; Zhang, X.; Du, B. Thermosensitive Ionic Microgels via Surfactant-Free Emulsion Copolymerization and in Situ Quaternization Cross-Linking. *ACS Appl. Mater. Interfaces* **2014**, *6*, 4498−4513.
(27) Zhou, X.; Nie, J.; Wang, Q.; Du, B. Thermosensitive Ionic Microgels with pH Tunable Degradation via in Situ Quaternization Cross-Linking. *Macromolecules* **2015**, *48*, 3130−3139.
(28) Jeronimo, P. C. A.; Araujo, A. N.; Montenegro, M.; Pasquini, C.; Raimundo, I. M. Direct Determination of Copper in Urine Using a Sol-Gel Optical Sensor Coupled to a Multicommutated Flow System. *Anal. Bioanal. Chem.* **2004**, *380*, 108−114.
(29) Saebel, C. E.; Shepherd, J. L.; Siemann, S. A Direct Spectrophotometric Method for the Simultaneous Determination of Zinc and Cobalt in Metalloproteins Using 4-(2-Pyridylazo)Resorcinol. *Anal. Biochem.* **2009**, *391*, 74−76.
(30) Engstrom, E.; Jonebring, I.; Karlberg, B. Assessment of a Screening Method for Metals in Seawater Based on the Non-Selective Reagent 4-(2-Pyridylazo)Resorcinol (PAR). *Anal. Chim. Acta* **1998**, *371*, 227−234.
(31) Vyshcherevich, I. V.; Kalinichenko, I. E. Photometric Determination in Drinking Water of Cobalt and Nickel with 4-(2-Pyridylazo)-Resorcinol. *J. Water Chem. and Technol.* **2010**, *32*, 33−38.
(32) Benee, L. S.; Snowden, M. J.; Chowdhry, B. Z. Novel Gelling Behavior of Poly(N-Isopropylacrylamide-co-Vinyl Laurate) Microgel Dispersions. *Langmuir* **2002**, *18*, 6025−6030.
(33) Schild, H. G. Poly (N-Isopropylacrylamide) - Experiment, Theory and Application. *Prog. Polym. Sci.* **1992**, *17*, 163−249.
(34) Schmidt, M.; Nerger, D.; Burchard, W. Quasi-Elastic Light-Scattering from Branched Polymers 0.1. Polyvinylacetate and Polyvinylacetate-Microgels Prepared by Emulsion Polymerization. *Polymer* **1979**, *20*, 582−588.
(35) Kuckling, D.; Vo, C. D.; Adler, H. J. P.; Volkel, A.; Colfen, H. Preparation and Characterization of Photo-Cross-Linked Thermosensitive PNIPAAm Nanogels. *Macromolecules* **2006**, *39*, 1585−1591.
(36) Cao, Z.; Du, B.; Chen, T.; Nie, J.; Xu, J.; Fan, Z. Preparation and Properties of Thermo-Sensitive Organic/Inorganic Hybrid Microgels. *Langmuir* **2008**, *24*, 12771−12778.
(37) Senff, H.; Richtering, W. Temperature Sensitive Microgel Suspensions: Colloidal Phase Behavior and Rheology of Soft Spheres. *J. Chem. Phys.* **1999**, *111*, 1705−1711.
(38) Senff, H.; Richtering, W. Influence of Cross-Link Density On Rheological Properties of Temperature-Sensitive Microgel Suspensions. *Colloid Polym. Sci.* **2000**, *278*, 830−840.
(39) Ghasemi, J.; Peyman, H.; Meloun, M. Study of Complex Formation Between 4-(2-Pyridylazo) Resorcinol and Al^{3+}, Fe^{3+}, Zn^{2+}, and Cd^{2+} Ions in an Aqueous Solution at 0.1 M Ionic Strength. *J. Chem. Eng. Data* **2007**, *52*, 1171−1178.
(40) Yusof, N. A.; Ahmad, M. Development of a Flow-Through Optosensor for Determination of Co(II). *Spectrochim. Acta, Part A* **2008**, *69*, 413−418.
(41) Pease, B. F.; Williams, M. B. Spectrophotometric Investigation of the Analytical Reagent 1-(2-Pyridylazo)-2-Naphthol and Its Copper Chelate. *Anal. Chem.* **1959**, *31*, 1044−1047.
(42) Anderson, R. G.; Nickless, G. Heterocyclic Azo Dyestuffs in Analytical Chemistry-A Review. *Analyst* **1967**, *92*, 207−238.
(43) Liu, T.; Li, G.; Zhang, N.; Chen, Y. An Inorganic-Organic Hybrid Optical Sensor for Heavy Metal Ion Detection Based on Immobilizing 4-(2-Pyridylazo)-Resorcinol on Functionalized HMS. *J. Hazard. Mater.* **2012**, *201*, 155−161.
(44) Xie, Y.; Bai, F. Y.; Li, J.; Xing, Y. H.; Wang, Z.; Zhao, H. Y.; Pu, Z. F.; Ge, M. F.; Shi, Z. Synthesis, Crystal Structure and Photoelectric Property of Two New Coordination Polymers Constructed by Longer-Spanning Suberic Acid and 4,4′-Bipyridine Ligands. *Spectrochim. Acta, Part A* **2010**, *77*, 749−754.
(45) Calzaferri, G.; Rytz, R. Electronic-Transition Oscillator Strength by the Extended Huckel Molecular-Orbital Method. *J. Phys. Chem.* **1995**, *99*, 12141−12150.
(46) El-Safty, S. A.; Ismail, A. A.; Matsunaga, H.; Nanjo, H.; Mizukami, F. Uniformly Mesocaged Cubic Fd3 mL Monoliths as Modal Carriers for Optical Chemosensors. *J. Phys. Chem. C* **2008**, *112*, 4825−4835.
(47) Aragay, G.; Pons, J.; Merkoci, A. Recent Trends in Macro-, Micro-, and Nanomaterial-Based Tools and Strategies for Heavy-Metal Detection. *Chem. Rev.* **2011**, *111*, 3433−3458.
(48) Ali, E. M.; Zheng, Y.; Yu, H. H.; Ying, J. Y. Ultrasensitive Pb^{2+} Detection by Glutathione-Capped Quantum Dots. *Anal. Chem.* **2007**, *79*, 9452−9458.

DOI: 10.1021/acsami.5b06653
ACS Appl. Mater. Interfaces 2015, 7, 21966−21974